e-Journal of Nondestructive Testing - ISSN 1435-4934 - www.ndt.net

EWSHM 2024
11th European Workshop on Structural Health Monitoring

Crack Tip Localization in Adhesively Bonded CFRP-CFRP Joints subjected to Mode II Fatigue Loading

Alessandra PANERAI [1], Benedetta ONEDA [1], Andrea BERNASCONI [1], Michele CARBONI [1]
[1] Department of Mechanical Engineering, Politecnico di Milano, Via La Masa 1, 20156 Milano, Italy
(michele.carboni@polimi.it)

Abstract. The use of resin-based composite materials in place of metals has gained prominence across various industries. Such composites offer a superior strength-to-weight ratio, addressing the increasing demand for lightweight structures to reduce emissions. As such, structural joining of composite materials is of growing importance. Traditional fasteners, however, not only compromise weight savings, but also introduce weak points within the structure. Adhesive bonding emerges as the most promising joining technology, balancing weight efficiency and performance. However, its broader adoption for primary structural joints is hindered by a lack of standardization of quality control and non-destructive inspection techniques and concerns about long-term reliability.

To address this challenge, the “CERTBOND” COST Action (CA18120) initiative was established to investigate adhesive bonding and develop a reliable certification roadmap for bonded primary structures. As part of this initiative, a Mode II fatigue loading Round Robin study was conducted on adhesively bonded CFRP-CFRP End-Notched Flexure specimens. While conducting the fatigue tests, supplementary techniques for estimating the crack tip position were employed. The selected techniques included visual testing (employing two different methods), ultrasonic phased array testing, and distributed strain sensing using optical backscatter reflectometry. The present study describes, compares and discusses the results obtained by the cited localization techniques.

Keywords: Adhesive joints, End Notched Flexure Specimens, Unidirectional reinforced Composites, Mode II fatigue loading.

Introduction

Adhesive bonding is the preferred joining method for composite materials, as it can provide a lighter and easier way to manufacture joints without needing to drill holes in the material [1,2]. These joints can be subjected to fatigue loads during service, so it is important to ensure their long-term safety. While many works have studied crack propagation under mode I loading conditions [3–5], recognized as the most critical [6], research on mode II crack propagation remains limited. Monitoring crack propagation under mode II loading presents

Media and Publishing Partner
https://doi.org/10.58286/29671

a number of challenges, as it is difficult to correctly locate the crack tip position due to the lack of opening between the two crack surfaces, leading to potentially inaccurate results. To address this challenge, the "CERTBOND" COST Action (CA18120) organized a Round Robin on fatigue crack propagation of adhesively bonded CFRP-CFRP joints under mode II loading.

Current standards on mode II crack propagation recommend Visual Testing (VT) and Compliance Monitoring (CM) to measure crack length during mode II fatigue tests. However, several works report that these methods may not always provide reliably accurate results. The use of alternative, or supplemental techniques may aid in providing a more precise measurement. Furthermore, the development of monitoring and non-destructive inspection techniques applicable to real-world joint applications is of great importance. Recognizing the significance of this topic, this study aims to compare and evaluate various techniques for locating cracks in composite adhesively bonded joints subjected to mode II fatigue load.

1. Materials and Methods

1.1 Specimen Preparation

Two rectangular End Notched Flexure (ENF) specimens were used, made of two layers of HexPly 8552 Unidirectional Carbon prepregs [7] bonded by FM 300 modified epoxy film adhesive [8] by Solvay. The specimens and their nominal dimensions are reported in Figure 1. When bonding the specimens, a 50 mm long PTFE (Teflon) insert was placed on one side as a crack starter.

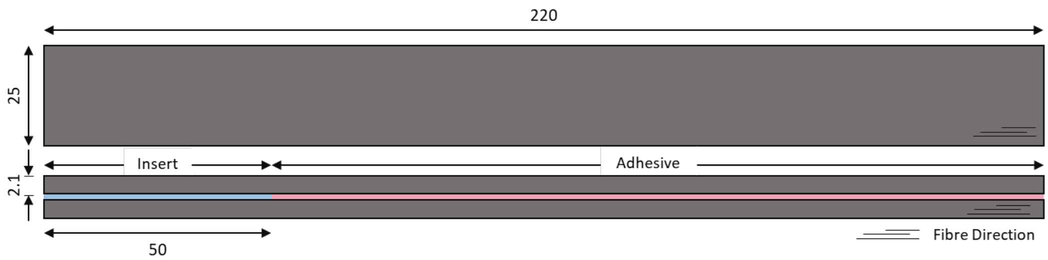

Figure 1: Scheme of the adopted ENF specimen. All dimensions in mm.

One lateral side of the specimens was sanded with 2500 grit sandpaper and polished with 6- and 1-μm diamond pastes so that it could be inspected by a microscope. The other lateral side was coated by a thin layer of white paint. A printed scale was attached to both sides.

High-definition low bending loss optical fibres were bonded on the lower surface of the specimens using 3M DP-490 adhesive. The fibre was connected to an optical backscattered reflectometry (OBR) interrogator ("ODiSI-B" by Luna Innovation Inc.). The adopted system allows a spatial resolution of 0.625 mm and an acquisition frequency of 23.7 Hz. Multiple measuring paths were obtained across the width of the specimens by bending the fibres, as shown in Figure 2.

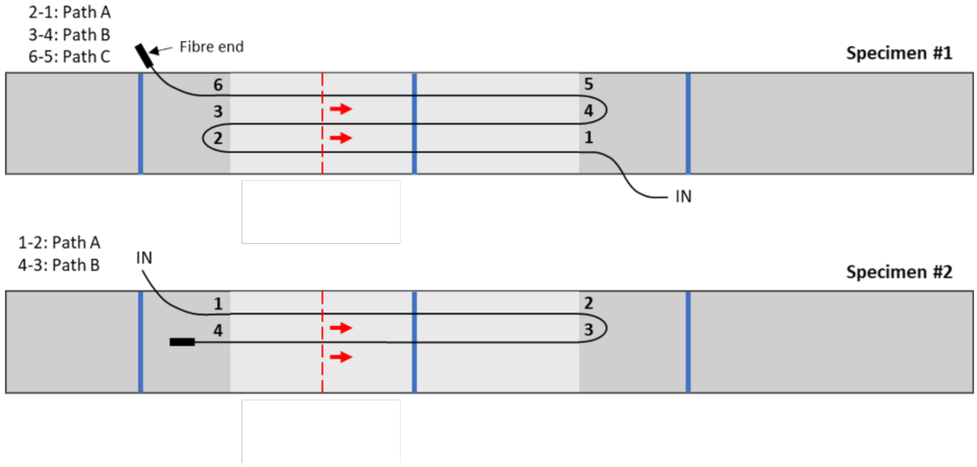

Figure 2: Fibre Paths in each specimen. The blue vertical lines indicated the position of the rollers during fatigue testing. The red vertical line indicates the initial crack tip position.

1.2 Testing Procedure

Specimens were precracked quasistatically. in a 3-point bending configuration by an MTS Landmark servo-hydraulic testing machine with a maximum load capacity of 25 kN, as shown in Figure 3. The specimens were positioned in the testing machine so that the tip of the PTFE foil was at 35 mm from the left roller and loaded in displacement control with a speed of 5 mm/min until a load drop, associated with precrack initiation and propagation, was registered. Specimens were then repositioned in the machine so that the new crack tip was again at 35 mm from the left roller. Fatigue testing was performed in displacements control at 5 Hz and with R=0.1.

(a) (b)

Figure 3: (a) 3-point bending setup and (b) fatigue testing setup

VT was performed on both sides of the specimens. The polished side was inspected with a 2 Megapixel Allied Vision Manta CCD microscope at 40x magnification, while the white painted side was inspected directly without any magnification. VT was always performed when the specimens were loaded.

Fatigue testing was stopped at planned intervals to perform a monotonic loading ramp, with a speed rate of 10 mm/min. Force and displacement were recorded to measure the specimens' compliance. Once the maximum fatigue displacement had been reached, it was held for some time so that VT could be carried out and the backface strain could be recorded by the OBR system. Then, the specimens were unloaded and taken out of the machine for phased array ultrasonic testing (PAUT).

PAUT was performed using an M2M Mantis control unit by Eddyfy Technologies equipped with a 10 MHz, 32 elements linear probe operated in pulse-echo mode and applying a linear scan (L-Scan) inspection and visualization. Real-time analysis and post-processing were performed by using M2M Capture software (v. 2020). A water-based silicon coupling agent was used between the probe and the surface of the piece. After performing PAUT, the specimen was carefully repositioned, and the fatigue test resumed.

2 Results and Discussion

For compliance monitoring, a cubic relationship (1) is fitted between compliance and crack length, according to Timoshenko's beam theory [9,10]. After precracking, the two constants C_1 and C_0 were obtained by placing the specimen on the 3-point bending setup to obtain three different crack lengths and measuring the compliance. These constants were then used to determine the crack length during fatigue testing.

$$C(a) = C_1 a^3 + C_0 \tag{1}$$

Two different strategies were employed to perform VT. Figure 4a shows a representative example of crack tip localization using the microscope. The cracked adhesive appears lighter in colour due to stress whitening [11]. This phenomenon was used to identify the crack tip, which was localized at the boundary between the whitened and the visually undamaged adhesive. This boundary, however, was not always very clear, and it was found that this method was often very sensitive to subjective interpretation.

Figure 4b shows a representative example of crack tip localization using white paint VT. Despite the lack of an opening between the two crack surfaces, the crack is visible thanks to the contrast with the white paint.

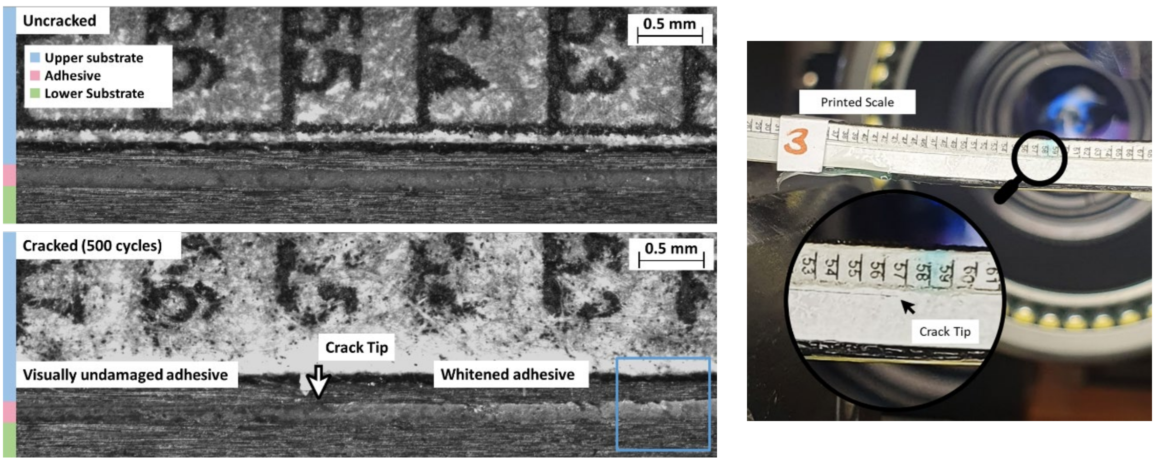

(a) (b)

Figure 4 (a) Visual testing using a microscope. (b) Visual testing aided by white paint.

To measure the crack length with PAUT, the centre of the sensor was marked, then the probe was positioned on the top side of the specimen, and moved until the crack tip was located under the middle of the probe. The crack length could then be read from the scale on the specimen, as shown in Figure 5a. Figure 5b shows an L-Scan representing the ultrasonic cross-section view of the specimen. The bonded side is characterized by two reflections, one due to the adhesive layer, and one due to the backwall echo of the further adherend. On the cracked side the ultrasonic beam is completely reflected by the crack surface. The boundary between these two regions marks the crack tip location.

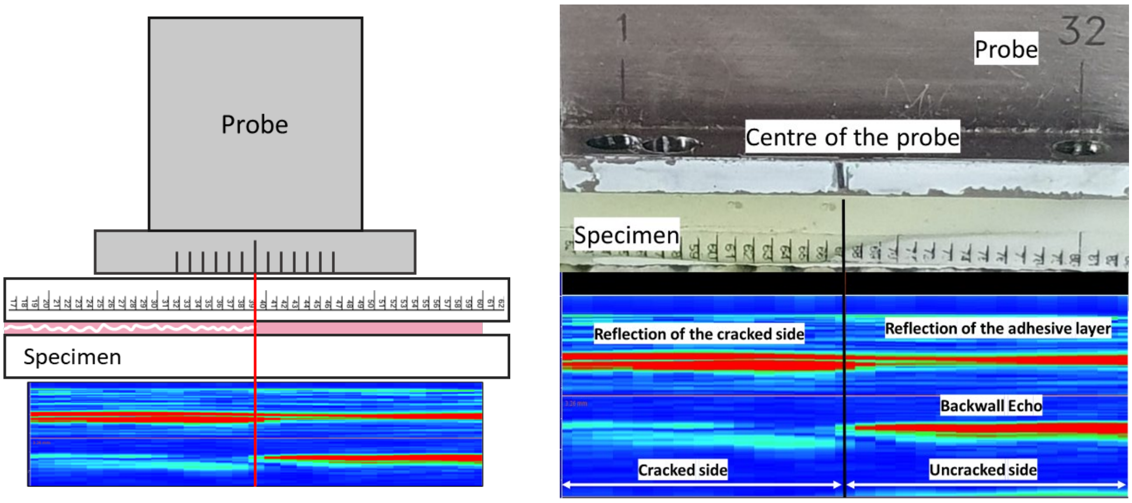

(a) (b)

Figure 5 Crack tip detection using PAUT.

Figure 6a shows the backface strain profile at the beginning of the tests. The different paths have very similar trends, indicating a straight crack front. The crack tip position is highlighted, and the first derivative of the signal is also shown. It can be observed that the crack tip can be localized by the minimum in the derivative, i.e. the inflection point. During the fatigue tests, the backface strain profiles evolve as a result of crack propagation (see Figure 6b). The inflection point can be found in each acquisition and used to measure the crack length.

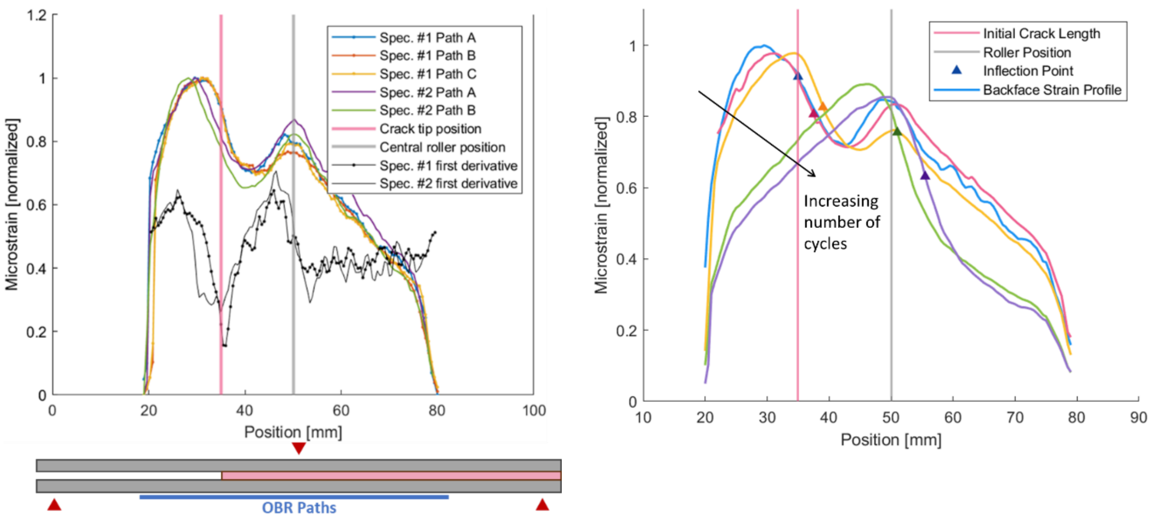

(a) (b)

Figure 6: (a) Backface strain profile at the beginning of the fatigue tests for both specimens. (b) Evolution of the backface strain profile during fatigue testing (specimen #2).

At the end of the tests, the specimens were opened to inspect the fracture surfaces (Figure 7). There is a marked difference in appearance between the fatigued adhesive and the final fracture, allowing to precisely measure the final crack length. The final crack front is quite uneven, so the final crack length was measured in three points: on each edge, and at its maximum, which occurred at some point in the middle of the specimens.

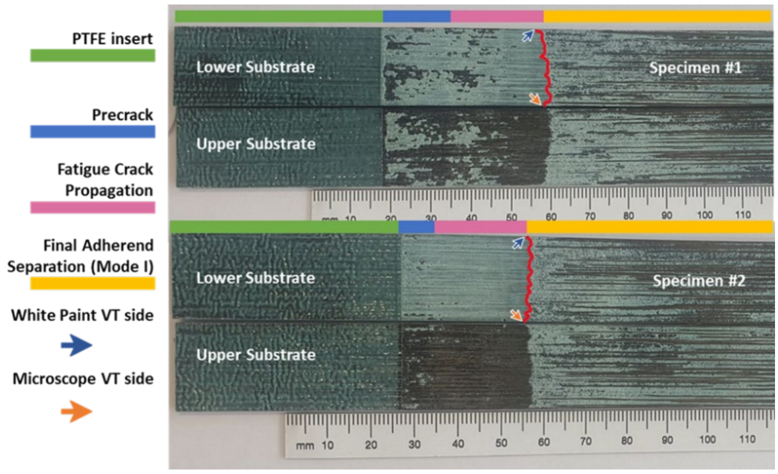

Figure 7: Fracture surfaces. The final crack front is highlighted in red.

In Figure 8 the different crack monitoring techniques are compared against each other. The final crack lengths are also reported.

The two VT techniques yielded different measurements throughout the tests. Microscope measurements were consistently longer than white paint for specimen #1, and consistently shorter for specimen #2. Comparison with the final crack profile indicated that they both accurately located the crack tip position on their respective edge, so the differences between them are likely due to the crack front growing unevenly rather than by either technique being biased. OBR and PAUT measurements were on average slightly higher than VT measurements, which is consistent with the shape of the crack profile. Between the two, OBR was more precise in identifying the final crack length.

On the other hand, CM consistently underestimates the crack length compared to all other techniques, and the final value obtained is quite lower than the observed final crack length. It appears that other phenomena besides crack propagation may be affecting the measured compliance, making this method unreliable. Indeed, other authors [12,13] have reported that the compliance method may not accurately account for the adhesive process zone, the friction of the rollers, and damage development within the substrates.

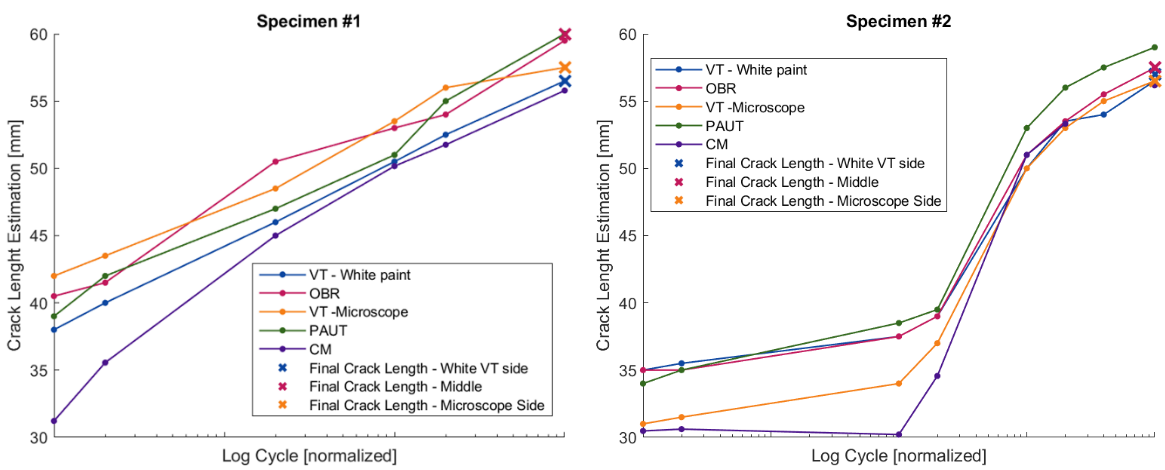

(a) (b)

Figure 8: Crack length estimation by the different techniques. (a) Specimen #1. (b) Specimen #2.

3 Conclusions

Five different techniques were applied to measure the crack tip position in composite adhesively bonded joints subject to mode II fatigue loading. The use of multiple monitoring techniques is recommended, as cracks grow in an uneven way, and have the tendency to be longer in the centre of the specimen than on the sides.

For this reason, it is advisable to perform VT on both sides of the specimens. Both VT techniques employed proved to be effective in identifying the crack tip position. However, using white paint to increase contrast is easier than direct observation of the adhesive, and does not necessarily require magnification. It remains that it is not possible to inspect the interior of the specimen by VT.

Both PAUT and OBR were successful in accurately measuring the crack length. The measurements provided by these two methods were quite similar between each other and to the final crack length in the middle of the specimen, while CM was found to not be a reliable monitoring method.

Acknowledgements

This research is performed in the frame of the experimental Round Robin for the characterization of the strength of adhesively bonded joints undertaken within the “CERTBOND” COST Action (CA18120) initiative “Reliable roadmap for certification of bonded primary structures”.

References

[1] Banea MD, da Silva LFM. Adhesively bonded joints in composite materials: An overview. Proceedings of the Institution of Mechanical Engineers, Part L: Journal of Materials: Design and Applications 2009;223:1–18. https://doi.org/10.1243/14644207JMDA219.

[2] Srinivasan DV, Vassilopoulos AP. Fatigue performance of wind turbine rotor blade epoxy adhesives. Polym Test 2023;121:107975. https://doi.org/10.1016/J.POLYMERTESTING.2023.107975.

[3] Moazzami M, Akhavan-Safar A, Ayatollahi MR, Poulis JA, da Silva LFM, Teixeira De Freitas S. A degradable mode I cohesive zone model developed for damage and fracture analysis of dissimilar composite/metal adhesive joints subjected to cyclic ageing conditions. Theoretical and Applied Fracture Mechanics 2023:104076. https://doi.org/10.1016/J.TAFMEC.2023.104076.

[4] Lima RAA, Tao R, Bernasconi A, Carboni M, Carrere N, Teixeira de Freitas S. Uncovering the toughening mechanisms of bonded joints through tailored CFRP layup. Compos B Eng 2023;263:110853. https://doi.org/10.1016/J.COMPOSITESB.2023.110853.

[5] Gorman JM, Thouless MD. The use of digital-image correlation to investigate the cohesive zone in a double-cantilever beam, with comparisons to numerical and analytical models. J Mech Phys Solids 2019;123:315–31. https://doi.org/https://doi.org/10.1016/j.jmps.2018.08.013.

[6] Pirondi A, Nicoletto G. Mixed Mode I/II fatigue crack growth in adhesive joints. Eng Fract Mech 2006;73:2557–68. https://doi.org/10.1016/J.ENGFRACMECH.2006.04.009.

[7] HexPly ® 8552 Epoxy matrix (180°C/356°F curing matrix) 2023.

[8] Ishai O, Rosenthal H, Sela N, Drukker E. Effect of selective adhesive interleaving on interlaminar fracture toughness of graphite/epoxy composite laminates. Composites 1988;19:49–54. https://doi.org/10.1016/0010-4361(88)90543-5.
[9] Morais AB de. Analysis of the fracture process zone and effective crack length in the adhesively bonded end-notched flexure specimen. J Adhes 2019;95:770–95. https://doi.org/10.1080/00218464.2018.1440214.
[10] Feng W, Moreira Arouche M, Pavlovic M. Fatigue crack growth characterization of composite-to-steel bonded interface using ENF and 4ENF tests. Compos Struct 2024:117963. https://doi.org/10.1016/J.COMPSTRUCT.2024.117963.
[11] Wei Y, Luo Q, Li Q, Sun G. On adhesively bonded joints with a mixed failure mode—An experimental and numerical study. Thin-Walled Structures 2023;192:110987. https://doi.org/10.1016/J.TWS.2023.110987.
[12] Renart J, Vicens J, Budhe S, Rodríguez-Bellido A, Comas J, Mayugo JA, et al. An automated methodology for mode II delamination tests under fatigue loading based on the real time monitoring of the specimen's compliance. Int J Fatigue 2016;82:634–42. https://doi.org/10.1016/J.IJFATIGUE.2015.09.021.
[13] Bieniaś J, Dadej K. Fatigue delamination growth of carbon and glass reinforced fiber metal laminates in fracture mode II. Int J Fatigue 2020;130:105267. https://doi.org/10.1016/J.IJFATIGUE.2019.105267.